J. Paleont. Soc. Korea. Vol. 22, No. 1, (2006) : p. 51-75

# PRESERVATION OF FOSSIL BONE FROM THE PIPE CREEK SINKHOLE (LATE NEOGENE, GRANT COUNTY, INDIANA, U.S.A.)

**James O. Farlow and Anne Argast**

*Department of Geosciences, Indiana-Purdue University, 2101 East Coliseum Boulevard, Fort Wayne, IN 46805, U.S.A.*

**Abstract:** The fossil assemblage from the Pipe Creek Sinkhole (PCS; Grant County, Indiana, USA) preserves abundant bones from a diversity of late Neogene, large and small, terrestrial and aquatic vertebrates. We used several techniques to investigate diagenesis of PCS bones: scanning electron microscopy, X-ray diffraction analysis, energy-dispersive X-ray analysis, and measurements of bone weight loss after ignition. Most PCS bone shows little surficial weathering. Internally PCS bone is also generally well-preserved, but at least one bone shows a small amount of cortical microbial attack. The chemistry of PCS bone is not unusual for fossil bone; the bone apatite is francolite. PCS bone shows small amounts of manganese and iron, both of which occur in greater abundance in sideritic fillings of bone pores, although most large openings in PCS bone remain unfilled by crystalline material. Microscopic, sideritic "hemispheroids" (often paired), probably of bacterial origin, abundantly occur on the trabecular surfaces of some PCS bone. Siderite is also abundant in numerous nodules in the otherwise unconsolidated PCS fossiliferous deposit. PCS bone apatite shows greater crystallinity than modern bone, with Full Width Half Maximum Values of the $d_{002}$ apatite peak comparable to those seen in bone from other paleontological sites.

**Key words:** Preservation, fossil bone, Pipe Creek Sinkhole, Neogene, Indiana

## INTRODUCTION

Shortly after death, vertebrate bones are subject to a host of physical, chemical, and biological processes that culminate either in the destruction or the fossilization of the bones (Rogers, 1924; Cook, 1951; Neill, 1957; Parker and Toots, 1980; Nriagu, 1983; Waldron, 1987; Williams and Potts, 1988; Newesley, 1989; Price, 1989; Locock *et al*., 1992; Bell *et al*., 1996a, b; Denys *et al*., 1996; Samoilov and Benjamini, 1996; Bocherens *et al*., 1997; Barker *et al*., 1997; Trueman and Benton, 1997; Downing and Park, 1998; Karkanas *et al*., 2000; Kohn and Cerling, 2002; Metzger *et al*., 2004; Carpenter, 2005; and see other references below). Bacteria, fungi, and protozoans attack bone for its organic content (mainly collagen; Hackett, 1981; Garland, 1987; Hanson and Buikstra, 1987; Piepenbrink, 1986, 1989; Grupe and Dreses-Werringloer, 1993; Child, 1995b; Nicholson, 1996; Davis, 1997; Jans *et al*., 2002). Some micro-organisms may spread from the dead animal's own digestive tract to bone tissues, traveling along the vascular system (Bell *et al*., 1996a). Bones buried in soil can also be attacked by the soil microflora (Child, 1995a). Micro-organisms not only degrade the organic component of bone, but may also destroy its mineral (apatite) fraction. Microbial bioerosion of bone may not occur immediately after death, but if microbial bone destruction does take place it does so early in diagenesis, and its effects are complete on a timescale of decades or centuries (Hedges and Millard, 1995; Hedges, 2002). When such bioerosion occurs, it probably most often results in complete destruction of the bone, and most buried bone is probably destroyed rather than fossilized (Nielsen-Marsh and Hedges, 2000; Trueman and Martill, 2002). Unlike relatively young bone in archaeological samples (Hedges and Millard, 1995), most older, fossil bone shows only minor effects of microbial attack (Hedges, 2002; Trueman and Martill, 2002; Chinsamy-Turan, 2005), suggesting that only those bones that never experience microbial bioerosion, or those in which microbial attack is halted by physical or chemical processes before it proceeds very far, can be-

come fossils (Trueman and Martill, 2002).

Dismemberment of carcasses by predators, or mechanical disarticulation of bones by flowing water, may isolate those bones from the gut region of the carcass, preventing the bones from being colonized by endogenous micro-organisms (Trueman and Martill, 2002). Bones buried in waterlogged soils may be less vulnerable to microbial bioerosion than bones in well-drained soils (Nicholson, 1996; Bocherens *et al*., 1997; Hedges, 2002), and staining of bones by humic acids or iron may also provide some protection (Garland, 1987; Hedges, 2002).

Abiotic factors also influence the survival of buried bone. Both low and high pH adversely affect bone preservation (Gordon and Buikstra, 1981; Henderson, 1987; Martill, 1991; Child, 1995a; Nicholson, 1996; Stephan, 1997; Denys, 2002; Hedges, 2002; Fernandez-Jalvo *et al*., 2002); slightly alkaline environments are best for bone survival. Warmer burial environments will accelerate whatever chemical or biological reactions affect a buried bone (Von Endt and Ortner, 1984; Henderson, 1987).

Recrystallization of bone mineral, and incorporation of new ions into the crystal structure of bone apatite, may begin at the same time as, or soon after, the organic fraction of bone is destroyed (Grupe and Piepenbrink, 1989; Tuross *et al*., 1989a, b; Ayliffe *et al*., 1994 Hubert *et al*., 1996; Pfretzschner 2000a, b, 2001, a, b, 2004). These changes, along with pore-filling by minerals, are strongly affected by abiotic physical and chemical soil environmental conditions (particularly groundwater chemistry) around a buried bone (Paine, 1937; Pate and Hutton, 1988; Stephan, 1997; Pfretzschner, 2000b; Trueman and Martill, 2002; Trueman *et al*., 2003; Clarke, 2004). Iron and manganese (Toots, 1963; Houston *et al*., 1966; Badone and Farquhar, 1982; Stephan, 1997) and fluorine (Rogers, 1924; Oakley, 1949; Brophy and Nash, 1968; Parker *et al*., 1974; Toots and Parker, 1979; Matsu'ura, 1982; Brinkman and Conway, 1985; Joshi and Kshirsagar, 1986; Chipera and Bish, 1991; Zocco and Schwartz, 1994; Hubert *et al*., 1996; Michel *et al*., 1996 Elorza *et al*., 1999; Quattropani *et al*., 1999; Trueman *et al*., 2003) are among the minerals commonly added to bone during fossilization.

Compared with "fresh" modern bone, fossil bone shows increased crystallinity (Schoeninger *et al*., 1989; Sillen, 1989; Tuross *et al*., 1989a, b; Chipera and Bish, 1991; Lee-Thorp and van der Merwe, 1991; Ayliffe *et al*., 1994; Zocco and Schwartz, 1994; Hedges and Millard, 1995; Person *et al*., 1995, 1996; Hubert *et al*., 1996; Michel *et al*., 1996; Sillen and Parkington, 1996; Elorza *et al*., 1999; Quattropani *et al*., 1999; Lee-Thorpe, 2002; Reiche *et al*., 2002, Smith *et al*., 2002), reflecting changes in apatite crystallite size and strain, as well as incorporation of F into, and loss of $CO_3$ from, the apatite crystal structure. Crystallinity can increase in bones exposed on the surface of the ground for several years (Tuross *et al*., 1989), but a time scale of millennia is generally necessary for much crystallinity change in buried bone (Sillen, 1989). Warmer burial temperatures probably result in increased crystallinity, as do other diagenetic modifications of bone (Hedges, 2002). Tooth enamel shows less change in crystallinity between modern and fossil specimens than does bone (Ayliffe *et al*., 1994; Michel *et al*., 1996).

The Pipe Creek Sinkhole (PCS; Grant County, Indiana, USA) preserves an abundant and diverse assemblage of plants and animals of Late Miocene or Early Pliocene (Late Hemphillian) age (Holman, 2000, 2003; Farlow *et al*., 2001; Martin *et al*., 2002). Here we characterize the geochemistry of PCS fossil bone, and from it reconstruct the chemical paleoenvironment in which PCS bones were preserved. We also compare the crystallinity of PCS bone with that of modern bone, and also with archaeological and paleontological bone samples of varying age.

In a symposium volume concerned mainly with Mesozoic vertebrates, our contribution may seem the odd man out. However, the chemistry of vertebrate bone is fairly uniform, and for continental vertebrates the taphonomic and diagenetic changes affecting bones after an animal's death should be similar, regardless of whether that animal was a turtle, a mammal, or a dinosaur.

## MATERIALS AND METHODS

The Pipe Creek Sinkhole (Fig. 1) was created by collapse of the roof of a cave developed in limestone reef rock (Farlow *et al*., 2001). Breakdown boulders floored the base of the sinkhole, above which were deposited alluvial fan sediments composed of locally-derived, reworked terra rossa silts and clays, clasts of limestone and chert, and sapropel, as well as quartzite pebbles of more distant provenance. At least once a pond developed in the sinkhole, lasting long enough to accumulate abundant fossils of freshwater charophytes and other plants, ostracodes, molluscs, small fishes, frogs, turtles, and water snakes.

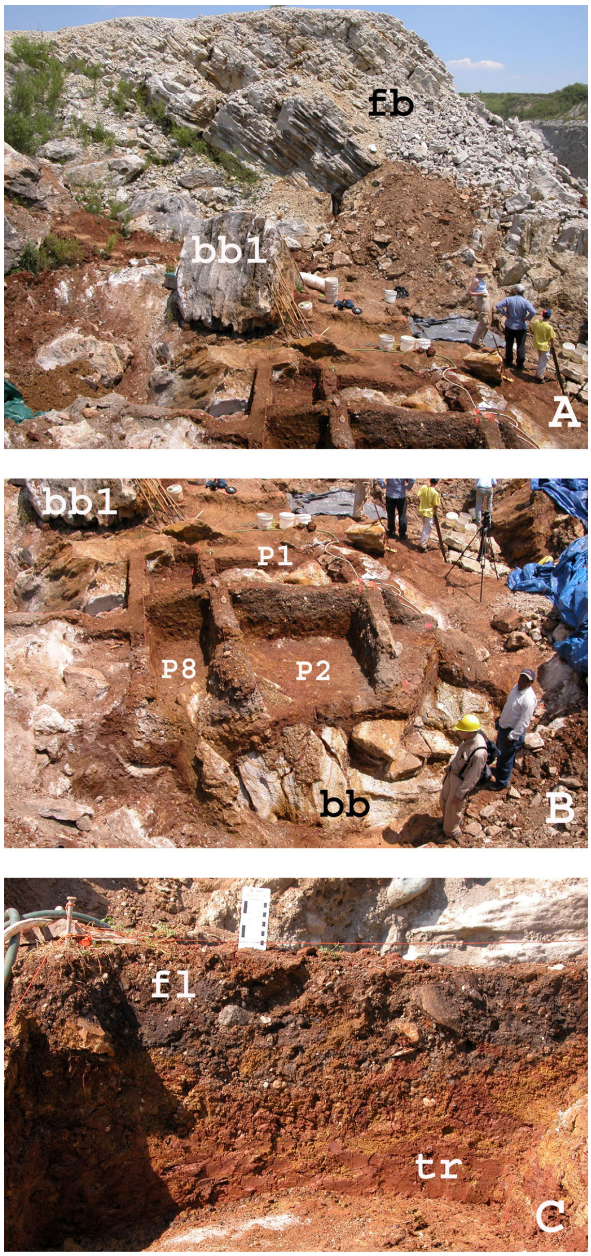


**Fig. 1.** The Pipe Creek Sinkhole, Grant County, Indiana, USA, July 2004. **A,** Overall structure; view to the east. The sinkhole was created by collapse of a cave developed in limestone flank beds (**fb**) of a Silurian reef. Prior to quarrying, such flank beds completely surrounded the sinkhole. After collapse of the cave roof, breakdown boulders (e.g. **bb1**) and unconsolidated sediment filled the sinkhole. Eventually the sinkhole and its deposits were buried beneath Pleistocene glacial till, which was stripped away in the initial stages of quarrying. **B,** View of the sinkhole floor, still looking to the east; bb1 is the same breakdown boulder seen in part A of this figure. Other breakdown boulders (**bb**) form a jumbled layer beneath the sinkhole's unconsolidated sediments. Although most of the sinkhole's sediments were removed by quarrying before geologists were able to study them, enough remained in situ of the late Neogene portion of the deposit to permit reconstruction of its stratigraphy. Sediments were removed from pits (**P1** = Pit 1, **P2** = Pit 2, **P8** = Pit 8), separated by baulks, for screen-washing. **C,** East-facing wall of Pit 1 showing typical disposition of unconsolidated sediments; terra rossa (**tr**) underlies the darker-colored fossiliferous layer (**fl**). The fossiliferous layer differs from the terra rosa in having a higher organic content (including the fossils).

Additional fossils represent a diversity of non-aquatic plants, reptiles, and large and small mammals. The fossiliferous deposit is largely unconsolidated, apart from abundant quartz/siderite nodules of varying size (some of which incorporate fossil bone or plant material; Fig. 2A).

Few PCS large mammal bones were found in articulation or association; most were isolated occurrences. Most large bones are broken, with unabraded broken edges; breakage may have been due to distortion of the cohesive, fine-grained, pond deposits under their own weight or that of overlying sediments (Fig. 2B, C). Because they were mostly collected by screen-washing, the degree of articulation and association of microvertebrate bones is unknown.

Taphonomic and diagenetic biases against preservation of small bones (Behrensmeyer *et al.*, 1979; Damuth, 1982; Von Endt and Ortner, 1984; Waldron, 1987; Nicholson, 1996) notwithstanding, the PCS vertebrate assemblage is numerically dominated by small bones, particularly of frogs and turtles, and to a lesser extent snakes and rodents. Most small bones show little surface weathering, and the few that have been sectioned thus far are also well-preserved internally (Fig. 3), retaining growth lines (in bones of reptiles and amphibians) and details of the bone cellular structure. Many large bones also show little surface

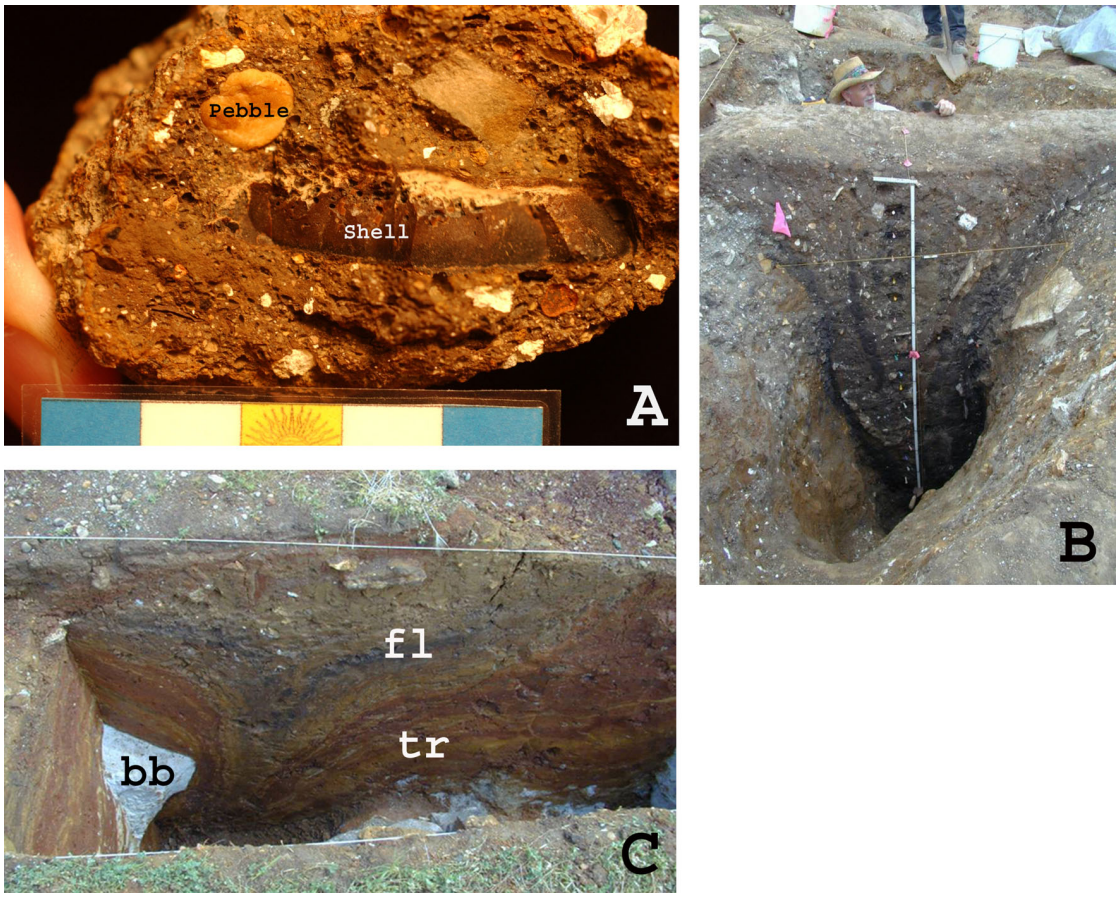


**Fig. 2. A**, Siderite/quartz nodule from Pipe Creek Sinkhole; centimeter scale at base of photograph. Note piece of turtle shell and a rounded quartzite pebble, along with other clasts incorporated into the nodule. **B-C**, Distortion of unconsolidated beds. **B**, Sediments sagging into a sinkhole drainage conduit; note nearly vertical orientation of large clasts. **C**, Sediments sagging around the margin of a limestone breakdown boulder (**bb**); **fl** = fossiliferous layer; **tr** = underlying terra rossa.

**Fig. 3.** Cross section through the ilial shaft (left) and dorsal ilial crest (right) of a Pipe Creek Sinkhole frog from the *Rana pipiens* complex. Scale bar = 1 mm.

weathering. However, even though the fragmentary nature of most PCS large mammal bones makes quantitative assessment problematic, a higher proportion of larger than of smaller bones show possible indications of pre-burial surface weathering (removal of cortical bone, particularly at articular surfaces, and possibly a more bleached color).

Most PCS bones are varying shades of moderate to dark brown (hue 5 or 10 YR, value 2-5, chroma 2-4; Geological Society of America [Munsell] Rock-Color Chart), but some bones are lighter in color (10 YR 6/6-8/2), possibly reflecting pre-burial weathering or small-scale, post-burial differences in groundwater and/or sediment chemistry around lighter as opposed to darker bones. Large voids and trabecular spaces within PCS bones are generally empty, unfilled by crystalline material.

## METHODS

We cut sections from PCS frog limb and girdle bones, pond turtle and tortoise shell fragments, rodent incisors, a worn ungulate tooth (possibly a lower incisor of a small male rhinoceros, a large camel incisor, or a peccary canine), and a fragmentary piece of probable rib from a large mammal (Tables 1, 2). For comparative purposes we also cut sections from a modern frog limb bone, turtle shells, a rodent bone and tooth, a deer and a peccary tooth, and a deer rib.

Samples of modern and PCS bones and teeth were examined under a scanning electron microscope (SEM) and subjected to X-ray diffraction (XRD) analysis. The same samples were examined by energy dispersive X-ray (EDX) analysis, and measurements of weight loss during ignition (LOI). Because turtle shell is among the most abundant bone material found in the PCS assemblage, we also did comparative XRD and LOI measurements on turtle shell from archaeological and paleontological sites of varying ages and paleoenvironmental contexts.

Where possible, we selected extant species that were the same as, or closely related to, PCS taxa in all our analyses. For example, painted turtle (*Chrysemys picta*), slider turtle (*Trachemys scripta*), Blanding's turtle (*Emydoidea blandingii*) and snapping turtle (*Chelydra serpentina*) or very similar species have all been identified in the PCS biota (Farlow *et al*., 2001), and modern and other fossil samples of these species were preferentially selected for comparison with PCS turtle shell.

**Energy Dispersive X-ray Spectroscopy (EDX) and Scanning Electron Microscopy** In 2003 we did pilot runs on a survey set of both modern and PCS bone (Table 1). Our analytical technique improved with experience, and in 2004 we did more intensive analyses on a smaller number of PCS and modern bones

**Table 1.** Energy dispersive X-ray (EDX) elemental analyses (weight percentage) of modern and Pipe Creek Sinkhole bones made during pilot runs in 2003. These data may not be as accurate or precise as our subsequent, more definitive determinations (Table 2), but because they were made on specimens not re-analyzed in our later runs they are reported here for comparative purposes. N = number of determinations done for a particular specimen.

| Taxon | Specimen (specimen ID, nature of material, provenance) | Mean Weight Percentage | | | | Other Elements[1] |
|---|---|---|---|---|---|---|
| | | Ca | P | O | F | |
| **Modern Bones and Teeth** | | | | | | |
| *Chrysemys picta* (painted turtle) | 2002-1, shell, Dekalb County, IN (N = 2) | 32.07 | 15.58 | 50.53 | 0 | Na, Mg, Al, Cl |
| | 2002-2, shell, Noble County, IN (N = 2) | 31.93 | 14.78 | 51.33 | 0 | Na, Mg, Cl |
| Unidentified turtle | Shell, Noble County, IN (N = 2) | 33.29 | 15.65 | 49.93 | 0 | Na, Mg |
| *Marmota monax* (woodchuck) | Phalanx, Allen County, IN (N = 1) | 33.25 | 16.70 | 48.97 | 0 | Na, Mg |
| *Sciurus carolinensis* (squirrel) | Incisor, Dekalb County, IN (N = 1) | 30.93 | 18.44 | 47.52 | 0 | Na, Mg |
| Mean Values: | | 32.29 | 16.23 | 49.66 | 0 | |
| **Pipe Creek Sinkhole Bones and Teeth** | | | | | | |
| Frog | Tibiofibula cortex (N =1) | 35.91 | 16.18 | 43.80 | 3.02 | Mn, Fe |
| | Radioulna or tibiofibula in nodule (N = 1) | 33.39 | 14.70 | 45.21 | 3.40 | Mn, Fe |
| | Urostyle (N = 2) | 35.54 | 16.10 | 44.27 | 2.69 | Mn, Fe |
| | Scapula (N = 2) | 33.89 | 15.55 | 46.29 | 2.87 | Mn, Fe, Al |
| Small Rodent | Incisor A (N = 1) | 35.04 | 17.62 | 45.05 | | Mn, Fe |
| | Incisor B (N = 1) | 36.19 | 16.23 | 43.58 | 2.49 | Mn, Fe, Na, Al |
| Mean Values: | | 34.99 | 16.06 | 44.70 | | |

[1]Present in amounts of 1 % or less

(Table 2). For the 2004 data we made a systematic evaluation of precision and accuracy of our measurements, and so we consider the 2004 data to be more definitive than the 2003 data. However, because we did not repeat analyses on all the bones previously examined in 2003, for comparative purposes we will report the 2003 data on specimens that were not re-analyzed in 2004. Values of the elemental composition of bone samples were much the same for the two years.

Samples were prepared for EDX by mounting the specimens with epoxy on standard aluminum stubs or on a petrographic slide, incrementally polishing to a final 0.05 μm finish, and coating the polished specimens with carbon. These were mounted in an ISI DS-130 SEM and examined with either back-scattered electrons (BSE) or secondary electrons (SE) as appropriate. Typical accelerating voltages were 18.3 KeV, though a few samples were examined at higher or lower voltages.

EDX analyses were made with a Kevex Sigma system. Nearly all analyses were obtained using a standards method and 200 second counts. Analyses are reported on an H- and C-free basis and summed to 100 weight percent. Water, collagen and $CO_2$ cannot, therefore, be directly measured by the methods used for analysis.

**Table 2.** Energy dispersive X-ray (EDX) elemental analyses of modern and Pipe Creek Sinkhole bones made in 2004. All data are weight percentages summed to 100 % on a C- and H-free basis. "A" indicates that a few samples had a small, but measurable, content of the indicated element.

| Ca | P | O | F | Na | Mg | Al | Si | S | Mn | Fe |
|---|---|---|---|---|---|---|---|---|---|---|
| **Modern Bones** | | | | | | | | | | |
| *Rana* sp. (frog) limb bone, Allen County, IN (N of measurements = 10): | | | | | | | | | | |
| 37.38 | 18.58 | 42.30 | 0 | 0.30 | 0.64 | 0.13 | 0.25 | 0.42 | 0 | 0 |
| *Chrysemys picta* (turtle) shell specimen 2003-2, Dekalb County, IN (N of measurements = 9): | | | | | | | | | | |
| 37.54 | 15.98 | 44.31 | 0 | 0.55 | 0.55 | 0.38 | 0.28 | 0.42 | 0 | 0 |
| *Odocoileus virginianus* (deer) rib, northern Indiana (N of measurements = 10): | | | | | | | | | | |
| 35.82 | 17.91 | 44.00 | 0 | 0.78 | 0.83 | 0.24 | 0.30 | A | 0 | 0 |
| Mean Values: | | | | | | | | | | |
| 36.91 | 17.49 | 43.54 | 0 | 0.54 | 0.67 | 0.25 | 0.28 | A | 0 | 0 |
| **Pipe Creek Sinkhole Bones** | | | | | | | | | | |
| Frog limb bone (N of measurements = 7) | | | | | | | | | | |
| 37.36 | 15.99 | 41.69 | 3.34 | 0 | A | A | 0 | 0 | 0.47 | 1.04 |
| Pond turtle shell (N of measurements = 10): | | | | | | | | | | |
| 37.13 | 16.23 | 41.92 | 3.49 | 0 | 0 | 0 | 0 | 0 | 0.51 | 0.72 |
| *Hesperotestudo* sp. (tortoise) shell (N of measurements = 15): | | | | | | | | | | |
| 37.84 | 16.19 | 40.91 | 3.81 | A | A | 0 | 0 | 0.32 | 0.19 | 0.70 |
| Ungulate tooth (N of measurements = 8): | | | | | | | | | | |
| 36.27 | 15.76 | 43.58 | 3.62 | 0 | 0 | 0 | 0 | 0 | 0.42 | 0.35 |
| Large mammal ?rib; bone material (N of measurements = 42): | | | | | | | | | | |
| 38.02 | 16.17 | 41.21 | 3.41 | 0 | 0 | 0 | 0 | 0 | 0.39 | 0.80 |
| Large mammal ?rib; vermicular external edge of bone cortex (N of measurements = 15): | | | | | | | | | | |
| 38.81 | 16.90 | 39.74 | 3.53 | 0 | 0 | 0 | 0 | 0 | 0.46 | 0.66 |
| Large mammal ?rib; bone adjacent to sideritic hemispheroids (N of measurements = 14): | | | | | | | | | | |
| 38.49 | 16.31 | 40.39 | 3.36 | A | A | A | A | 0 | 0.40 | 0.85 |
| Mean Values[1] | | | | | | | | | | |
| 37.32 | 16.07 | 41.86 | 3.53 | A | A | A | A | A | 0.40 | 0.72 |
| **Siderite Associated with Pipe Creek Sinkhole Bone** | | | | | | | | | | |
| Material filling pore spaces in *Hesperotestudo* shell (N of measurements = 15): | | | | | | | | | | |
| 5.83 | 0 | 45.17 | 0 | 0 | 0.22 | 0 | 0 | 0 | 3.70 | 45.03 |
| Hemispheroids in interior of large mammal ?rib (N of measurements = 22): | | | | | | | | | | |
| 4.52 | 0.31 | 42.55 | 0 | 0 | 0 | A | 0 | 0 | 2.96 | 49.64 |
| Mean Values: | | | | | | | | | | |
| 5.17 | 0.15 | 43.86 | 0 | 0 | 0.11 | A | 0 | 0 | 3.33 | 47.33 |

[1]Calculated using only the first row of data for the large mammal ?rib

Fluorine can be directly measured using the thin window on the Kevex Sigma system; however, count rates are low and considerable error can be anticipated where low concentrations of fluorine occur in the presence of iron (due to interference of the F K-line with the Fe L-line), as it does in several of the samples. Similar problems occur where small Si concentrations occur in the presence of high P concentration. Aside from these special cases, accuracy and precision (2004 data) can be evaluated based on a set of 12 replicate analyses of standard almandine, 11 replicates of standard Cr-rich diopside (both completed after the analysis of the shells and bones) and 23 replicates of standard apatite (completed before, during and after the analysis of the shells and bones). These results are summarized in Table 3.

**X-ray Diffraction (XRD)** Samples were prepared for XRD by crushing in a percussion mortar and hand grinding with an agate mortar and pestle until reduced to a sufficiently fine powder. A few samples of modern turtle shell were very resistant to hand grinding. These were finished with a tungsten-carbide ball mill, run in one minute increments, with the finer powder (< 44 μm) removed at each interval by passing the sample through a sieve.

Diffraction patterns were prepared on a Philips APD3520/PW1729 diffractometer using a copper tube at 40 kV and 30 mA, theta compensating slit and graphite monochrometer. All samples were mounted using the randomly-oriented backpack method (e.g., Moore and Reynolds, 1997), scanned in steps of $0.005^{o}$ 2θ and smoothed using a 15-point weighted moving average. Six samples (PCS *Hesperotestudo* and modern *Chrysemys picta* shell, PCS ungulate tooth, modern deer (*Odocoileus virginianus*) and peccary (*Tayassu tajacu*) tooth, PCS large mammal ?rib and modern *O. virginianus* rib) were scanned from 20 to $60^{o}$ 2θ at 2 sec/step. All other samples were scanned from 24 to $35^{o}$ 2θ in 1 second steps. Most of these also included a fluorite internal standard.

Full Width at Half Maximum (FWHM) measurements were made on the apatite $d_{002}$ peak. This measurement has proven useful as a measure of apatite crystallinity (e.g Sillen, 1989), although Person *et al.* (1995, 1996) have objected to this approach due to the possible interference of quartz. The alternate proposed method for determining apatite crystallinity is complicated and involves the measurement of several apatite peaks that were poorly resolved or completely unresolved in our patterns and is therefore unworkable. The straight-forward approach of determining the FWHM of apatite $d_{002}$ is an appropriate measure of crystallinity when care is taken to monitor the operation of the diffractometer and sample compositions.

**Table 3.** Results of EDX replicate analyses. All data are in weight % summed to 100 wt. %. Standards and accepted values provided by Structure Probe, Inc. Measured values and standard deviations (SD) based on 12 replicates of almandine, 11 replicates of diopside, and 23 replicates of apatite.

| Material | O | F | Na | Mg | Al | Si | P | Ca | Cr | Mn | Fe |
|---|---|---|---|---|---|---|---|---|---|---|---|
| **Almandine**: | | | | | | | | | | | |
| Accepted | 42.01 | | | 6.45 | 11.67 | 18.32 | | 3.00 | | 0.46 | 18.09 |
| Measured | 42.53 | | | 6.05 | 11.52 | 18.55 | | 2.99 | | 0.39 | 17.98 |
| SD | 0.37 | | | 0.05 | 0.09 | 0.15 | | 0.08 | | 0.06 | 0.16 |
| **Diopside:** | | | | | | | | | | | |
| Accepted | 43.92 | | 0.33 | 10.34 | | 25.52 | | 18.23 | 0.34 | | 1.08 |
| Measured | 43.12 | | 0.36 | 10.61 | | 25.81 | | 18.11 | 0.97 | | 1.03 |
| SD | 0.66 | | 0.11 | 0.07 | | 0.25 | | 0.28 | 0.29 | | 0.08 |
| **Apatite:** | | | | | | | | | | | |
| Accepted | 38.07 | 3.77 | | | | | 18.42 | 39.74 | | | |
| Measured | 37.64 | 3.84 | | | | | 18.65 | 39.87 | | | |
| SD | 0.36 | 0.21 | | | | | 0.20 | 0.30 | | | |

We do, however, have some concern about the way FWHM data have been previously reported in the literature, as slit settings and other instrumental parameters that could affect peak width have not been routinely reported. Consequently we did nine replicate analyses of characteristically well crystallized Hot Springs Arkansas quartz along with the shell and bone samples. This quartz is widely available, and others wishing to compare their data with ours can run the same quartz as an internal standard. The nine replicates produced an average FWHM for quartz $d_{101}$ (~26.66° 2θ) of 0.16° 2θ with a standard deviation of 0.02° 2θ. This standard deviation provides a useful estimate for the precision of our FWHM measurements.

**Loss on Ignition (LOI)** LOI was determined on powders first used for XRD. Each sample was dried overnight at 105-110°C, weighed, fused for 3 hours at 500°C in alumina crucibles, and reweighed. The resultant weight loss was recast as weight % LOI. Heating samples at 500-550°C is sufficient to remove organic material but leaves apatite and carbonates unchanged. Oxidation of iron and loss of structural water from susceptible clay minerals may occur at these temperatures.

Replicates were determined for seven samples from the analytic set. One specimen, the PCS large mammal ?rib, was analyzed three times and showed unusually large scatter in the wt. % LOI. Results are summarized in Table 4.

**Institution Acronyms - INSM,** Indiana State Museum (Indianapolis); **IPFW**, Indiana-Purdue University Archaeological Survey, Fort Wayne, IN; **SMM**, Science Museum of Minnesota, Saint Paul, MN; **TMP**, Tyrrell Museum of Paleontology, Drumheller, Alberta; **USNM**, U.S. National Museum of Natural History (Smithsonian Institution, Washington, D.C.).

## RESULTS

### BONE ELEMENTAL COMPOSITION

Although the number of individual bones analyzed was too few for a definitive statement, both the 2003 and the 2004 data suggest slight increases in the wt % of Ca, and slight decreases in the wt % of P and O, between modern and PCS bone (Tables 1, 2). The theoretical Ca/P weight ratio of unweathered bone is 2.15 (White and Hannus, 1983), which is very close to our results for modern bone (Table 2). Our 2003 data for PCS bone show a comparable ratio (Table 1), but our possibly better 2004 PCS data indicate a Ca/P weight ratio of 2.3, suggesting some enrichment of Ca compared with modern bone. The modern bones had small amounts of Na, Mg, Al, Si, and S, and all of these could be found in some PCS bone samples.

**Table 4.** Results of loss on ignition (LOI) replicate analyses. LOI data in weight %. Information about the identity of turtle specimens provided in Table 5.

| Specimen | Replicate 1 | Replicate 2 | Replicate 3 |
|---|---|---|---|
| PCS large mammal ?rib | 6.4 | 4.1 | 4.8 |
| PCS ungulate tooth | 4.1 | 4.3 | ----- |
| PCS *Hesperotestudo* shell | 8.2 | 8.0 | ----- |
| Turtle B1 | 3.8 | 3.5 | ----- |
| Turtle B8 | 3.0 | 2.7 | ----- |
| Turtle B17 | 2.3 | 2.1 | ----- |
| Turtle D1 | 4.4 | 4.3 | ----- |

Fluorine was consistently present at 3-4 wt % in PCS bone; F routinely occurs at a few wt % in fossil bone (see references cited above, introduction). Francolite is the name given to apatite containing significant $CO_2$ and > 1 % F (e.g., Chang *et al*., 1998). It forms after bone is buried and porewater fluoride is incorporated into the original carbonated hydroxyl apatite (Berna *et al*., 2004). The $CO_3^{2-}$ content of francolite can be estimated by measuring the $\Delta 2\theta$ of the $d_{004}$ and $d_{410}$ diffraction peaks (Schuffert *et al*., 1990). Measurements for the PCS *Hesperotestudo* shell, large mammal ?rib, and ungulate tooth yield $CO_3^{2-}$ concentrations in the approximate range of 4-6 wt %. The $d_{410}$ peak was poorly resolved and estimates with greater attached precision are probably not warranted. These results are sufficient, however, to identify the PCS bone bioapatites as of the francolite variety.

PCS bone also differs from modern bone in consistently showing small amounts (< 1 wt %) of Mn and Fe. Although most pore spaces within PCS bone have not been filled with crystalline material, where such infilling has occurred (Fig. 4) it is chemically quite different from the bone itself; compared with the bone, the material filling pore spaces is low in Ca, P, and F, but high in Mn and especially Fe (Table 2; Fig. 5). X-ray diffraction indicates that much of the pore-filling material is siderite (Fig. 6A).

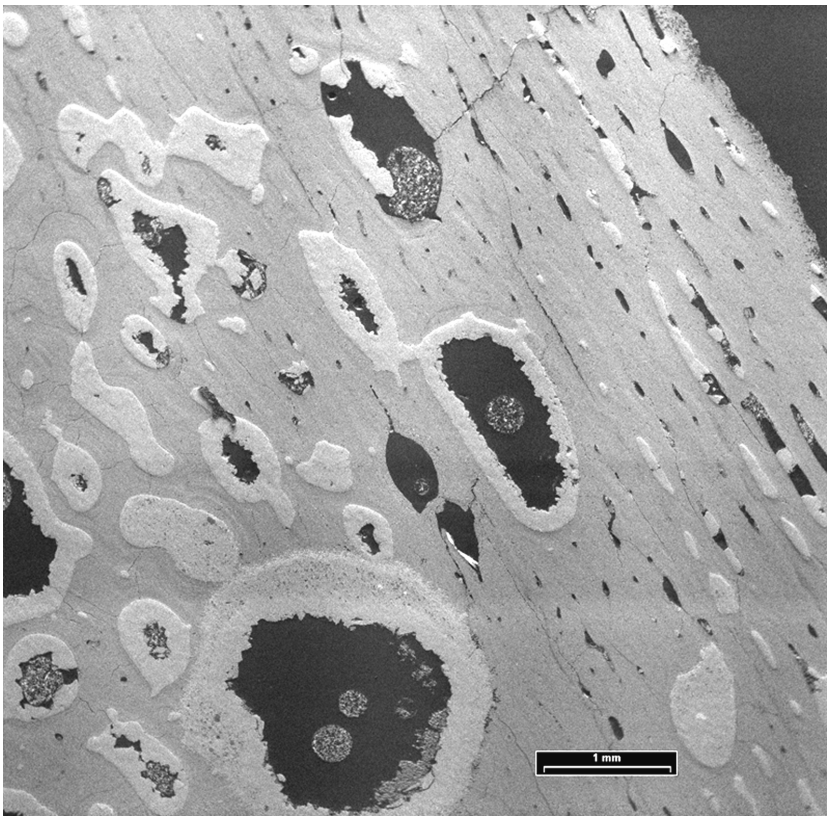


**Fig. 4.** Back-scattered electron image of a polished section through shell material of the extinct tortoise *Hesperotestudo* from Pipe Creek Sinkhole; scale bar = 1 mm. Many pore spaces are unfilled with crystalline material (black), but partial or complete filling of some spaces (light gray) can be seen. The bone itself in this image and in Fig. 5 is a darker shade of gray than the pore-filling material.

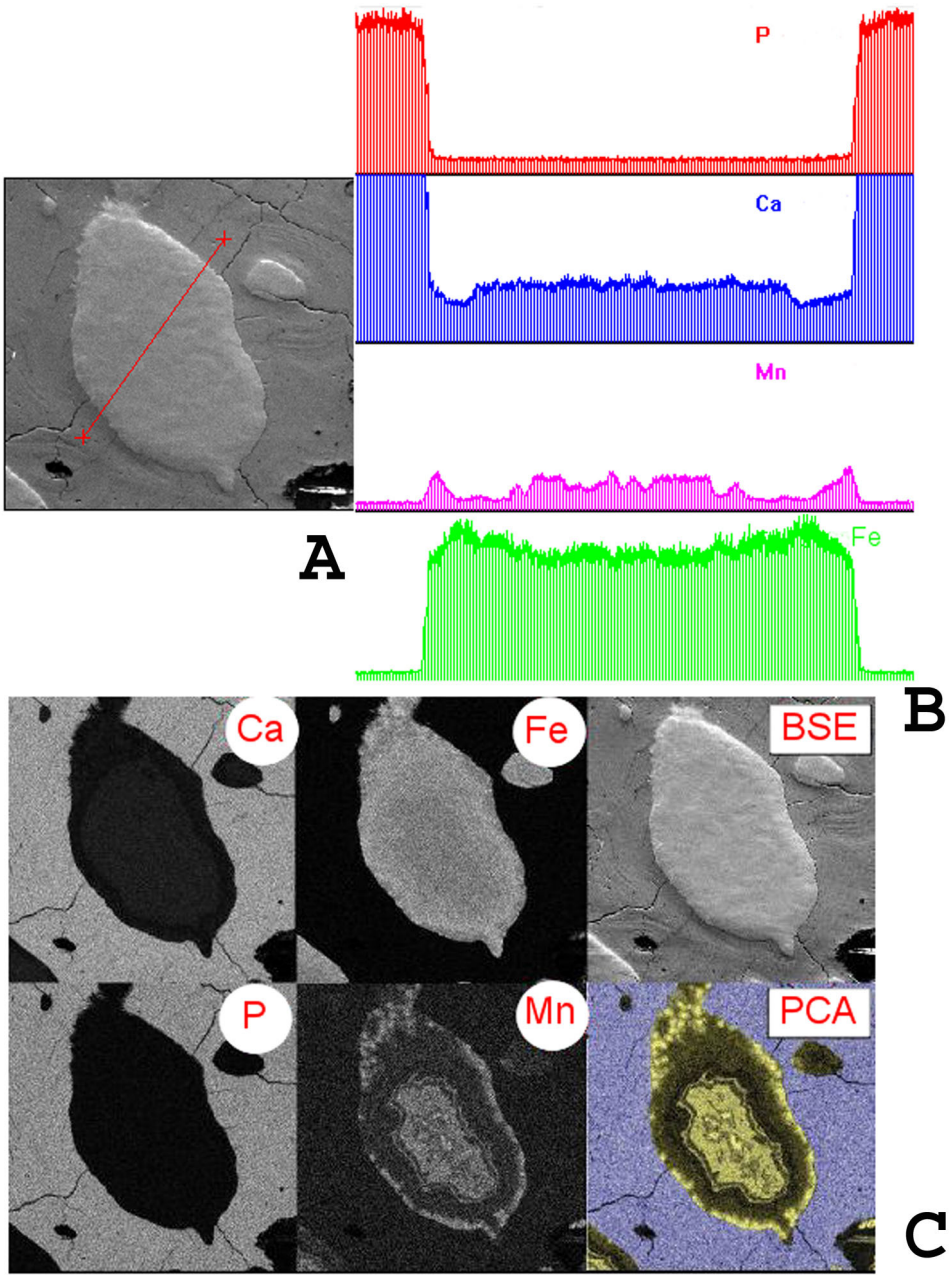


**Fig. 5.**Differences determined by energy dispersive X-ray spectroscopy in elemental composition between bone of the shell of *Hesperotestudo* and crystalline material filling pore spaces within the bone (cf. Fig. 4). **A**, Location of transect across crystal-filled bone pore. **B**, Relative proportions of phosphorus (red), calcium (blue), manganese (pink), and iron (green) along the transect; note high values of P and Ca in the bone outside the pore, and high values of Mn and especially Fe in the pore-filling material. **C**, X-ray maps (1024 * 1024 pixel matrix) of compositional differences inside and outside the bone pore. Brightness of each element image is proportional to the concentration of that element. Brightness of the back-scattered electron (BSE) image is proportional to the average atomic number of the material. The principal components analysis (PCA) emphasizes the compositional contrast between bone material and pore-filling material. Note the brightness (light shade) of Ca and P in the bone as opposed to the pore material (dark shade), and the brightness of Fe and Mn in the pore-filling material. The Mn and possibly Fe show compositional zoning of the pore-filling material, indicating a complex chemical history.

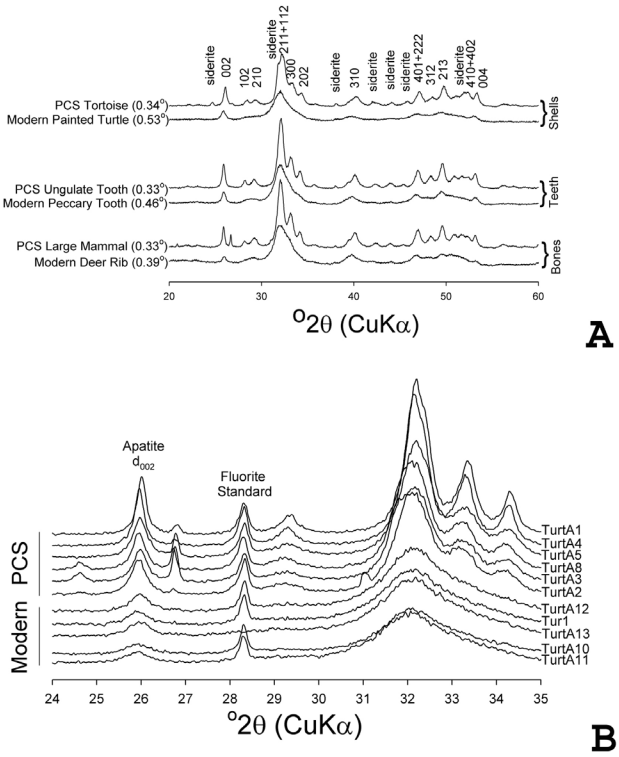


**Fig. 6.** X-ray diffraction patterns of Pipe Creek Sinkhole (PCS) and modern bone. **A**, Comparisons of chelonian shell, ungulate teeth, and mammal bones; information about each specimen is provided in Table 5. The painted turtle specimen is PTTUR-1, and the PCS tortoise is *Hesperotestudo.* The *Hesperotestudo* material includes both bone of the shell and crystalline material filling bone pore spaces. Diagnostic peaks for siderite are labeled by name, and selected peaks for apatite are labeled by number. Note the more sharply defined peaks of the PCS material than of their modern counterparts. **B**, similar but more detailed comparison of PCS and modern turtle shell; specimen information in Table 5. Note again the better defined peaks of PCS than of modern turtle shell, indicating greater crystallinity of bone apatite.

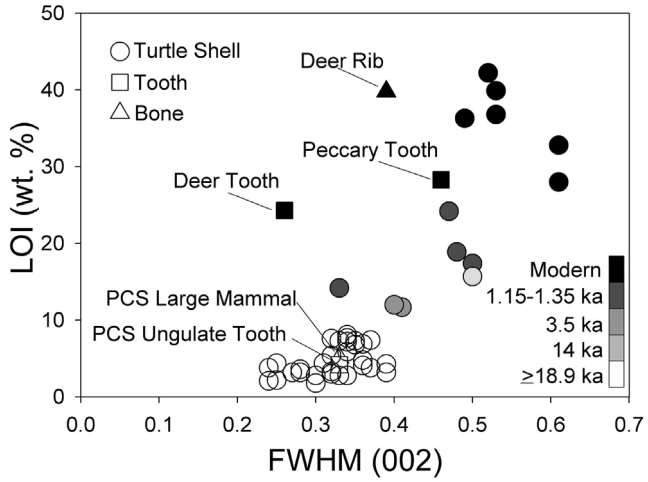


**Fig. 7.** Relationship between two parameters of bone diagenesis, loss on ignition (LOI) and Full Width at Half Maximum of the apatite $d_{002}$ X-ray diffraction peak (FWHM). FWHM is inversely related to bone apatite crystallinity; low values of FWHM indicate high crystallinity. The relationship between LOI and crystallinity is therefore negative.

## BONE CRYSTALLINITY

X-ray diffraction patterns (Fig. 6) indicate greater crystallinity of PCS than of modern bone, as is commonly observed in comparisons of Recent and fossil bone (see above-cited references). FWHM and LOI are positively correlated in bone of varying age (Table 5; Fig. 7); for turtle and tortoise shell material, the correlation is quite high ($r = 0.858$, $p < 0.001$). Because FWHM is inversely related to crystallinity, the latter is consequently inversely related to LOI. Furthermore, both LOI and FWHM appear to be related to

**Table 5.** Crystallinity (Full Width at Half Maximum of the $d_{002}$ apatite peak) of turtle and tortoise shell of varying ages, and of modern and Pipe Creek Sinkhole ungulate bone and tooth samples. Modern samples are assigned an arbitrary absolute age of 1 year. Ages of archaeological samples are based on radiocarbon dates (Holman and Richards, 1993; McCullough, 2005). Absolute ages of paleontological samples are estimates based on biostratigraphic and/or paleomagnetic correlation (Van Der Meulen, 1978; Dowsett and Wiggs, 1992; Ward, 1985; Ward and Powers, 1989; Woodburne, 2004). Where known, the taxon of turtle or tortoise is indicated; where possible, the turtle taxa from various faunas were the same as those known to occur at Pipe Creek Sinkhole (Farlow *et al*., 2001). UID = unidentified taxon. "Uncat" = uncatalogued specimen.

| Lab ID | Catalog Number | Locality | Stratigraphic Age | Absolute Age (Ka) | Taxon | FWHM | LOI (wt %) |
|---|---|---|---|---|---|---|---|
| Turtles and Tortoises | | | | | | | |
| TurtA10 | ----- | Allen Co., IN | Holocene | 0.001 | *Emydoidea blandingii* | 0.61 | 28.0 |
| TurtA11 | ----- | Allen Co., IN | Holocene | 0.001 | *Chelydra serpentina* | 0.61 | 32.8 |
| TurtA12 | 2003-7 | Dekalb Co., IN | Holocene | 0.001 | *Chrysemys picta* | 0.49 | 36.3 |
| TurtA13 | 2004-1 | Allen Co., IN | Holocene | 0.001 | *Chrysemys picta* | 0.53 | 39.9 |
| PTTUR-1 | 2002-1 | Dekalb Co., IN | Holocene | 0.001 | *Chrysemys picta* | 0.53 | 42.2 |
| Tur1 | 2002-2 | Noble Co., IN | Holocene | 0.001 | *Chrysemys picta* | 0.53 | 36.8 |
| TurtC1 | IPFW 04.83/667 | Castor Farm, Hamilton Co., IN | Holocene | 1.15 | *Chelydra serpentina* | 0.48 | 18.9 |
| TurtC3 | IPFW 04.83/667 | Castor Farm, Hamilton Co., IN | Holocene | 1.15 | *Chelydra serpentina* | 0.50 | 17.4 |
| TurtC4 | IPFW 04.83/937 | Castor Farm, Hamilton Co., IN | Holocene | 1.15 | *Apalone* sp. | 0.33 | 14.2 |
| TurtC2 | IPFW 04.62/1442 | Strawtown Enclosure, Hamilton Co., IN | Holocene | 1.35 | UID turtle | 0.47 | 24.2 |
| TurtE2 | INSM uncat | Prairie Creek, Daviess Co., IN Zone B LF2 Unit L-204 | Holocene | 3.5 | UID turtle | 0.41 | 11.7 |
| TurtE3 | INSM uncat | Prairie Creek, Daviess Co., IN Zone B LF1 Unit L-859 | Holocene | 3.5 | UID turtle | 0.40 | 12.0 |
| TurtE1 | INSM uncat | Prairie Creek, Daviess Co., IN Zone D Unit L-1497 | Pleistocene | 14 | UID turtle | 0.50 | 15.7 |
| TurtB2 | USNM 508573 | Ardis Local Fauna, Harleyville, Dorchester Co., SC | Pleistocene | 18.9 | *Emydoidea blandingii* | 0.35 | 6.8 |

**Table 5.** *Continued*.

| | | | | | | | |
|---|---|---|---|---|---|---|---|
| TurtB3 | USNM 508571 | Ardis Local Fauna, Giant Portland Cement Co., Harleyville, Dorchester Co., SC | Pleistocene | 18.9 | UID turtle | 0.33 | 7.3 |
| TurtB4 | USNM 508576 | Ardis Local Fauna, Harleyville, Dorchester Co., SC | Pleistocene | 18.9 | *Trachemys scripta* | 0.32 | 3.0 |
| TurtB5 | USNM 508580 | Ardis Local Fauna, Harleyville, Dorchester Co., SC | Pleistocene | 18.9 | *Chelydra serpentina* | 0.32 | 7.6 |
| TurtB12 | USNM 508575 | Ardis Local Fauna, Harleyville, Dorchester Co., SC | Pleistocene | 18.9 | *Trachemys scripta* | 0.32 | 5.4 |
| TurtB13 | USNM 508578 | Ardis Local Fauna, Harleyville, Dorchester Co., SC | Pleistocene | 18.9 | *Chrysemys picta* | 0.34 | 7.2 |
| TurtB16 | USNM 508579 | Ardis Local Fauna, Harleyville, Dorchester Co., SC | Pleistocene | 18.9 | *Chelydra serpentina* | 0.35 | 7.3 |
| TurtB19 | USNM 508574 | Ardis Local Fauna, Harleyville, Dorchester Co., SC | Pleistocene | 18.9 | *Chrysemys picta* | 0.34 | 7.7 |
| TurtB15 | USNM 508572 | Cumberland Cave, MD | Pleistocene | 800 | ?*Terrapene* | 0.34 | 5.9 |
| TurtB6 | USNM 508563 | Austin Pit, Timothy Creek, Dorchester Co., SC | Late Pliocene/Early Pleistocene | 1800 | UID turtle | 0.28 | 3.2 |
| TurtB11 | USNM 508565 | Glenns Ferry Fm, Hagerman, ID | Pliocene | 3000 | UID turtle | 0.34 | 2.8 |
| TurtB8 | USNM 508566 | Broadhurst Bridge area, Wayne Co., NC | ?Pliocene | ?3600 | UID turtle | 0.30 | 2.8 |
| TurtB18 | USNM 508568 | Martin Marietta Co., NC | Pliocene | ?3600 | UID turtle | 0.27 | 3.2 |
| TurtB7 | USNM 508570 | Yorktown Fm, Lee Creek Mine, Beaufort Co., NC | Pliocene | 3900 | UID turtle | 0.37 | 3.8 |
| TurtB9 | USNM 508567 | Yorktown Fm, Lee Creek Mine, Beaufort Co., NC | Pliocene | 3900 | UID turtle | 0.33 | 2.8 |
| TurtB14 | USNM 508569 | Yorktown Fm, Lee Creek Mine, Beaufort Co., NC | Pliocene | 3900 | UID turtle | 0.39 | 3.2 |
| TurtA1 | INSM uncat | Pipe Creek Sinkhole | Early Pliocene (latest Hemphillian) | 5000 | UID turtle | 0.24 | 3.8 |

**Table 5.** *Continued*.

| | | | | | | | |
|---|---|---|---|---|---|---|---|
| TurtA2 | ISNM uncat | Pipe Creek Sinkhole | Early Pliocene | 5000 | UID turtle | 0.39 | 4.3 |
| TurtA3 | INSM uncat | Pipe Creek Sinkhole | Early Pliocene | 5000 | UID turtle | 0.37 | 7.4 |
| TurtA4 | INSM uncat | Pipe Creek Sinkhole | Early Pliocene | 5000 | UID turtle | 0.25 | 4.4 |
| TurtA5 | INSM uncat | Pipe Creek Sinkhole | Early Pliocene | 5000 | UID turtle | 0.36 | 4.8 |
| TurtA8 | INSM uncat | Pipe Creek Sinkhole | Early Pliocene | 5000 | *Trachemys scripta* | 0.36 | 6.9 |
| Hesper | INSM uncat | Pipe Creek Sinkhole | Early Pliocene | 5000 | *Hesperotestudo* | 0.34 | 8.1 |
| TurtA9 | IPFW uncat | Love Bone Bed, Alachua Fm, Alachua Co., FL | Late Miocene (latest Clarendonian) | 9500 | UID turtle | 0.30 | 1.8 |
| TurtB17 | USNM 182424 | near Point Blank, San Jacinto Co., TX | Mid-Miocene (Barstovian) | 14,000 | UID turtle | 0.25 | 2.2 |
| TurtB20 | ----- | Poleside Member, Brule Fm | Oligocene | 32,500 | *Stylemys nebrascensis* | 0.24 | 2.1 |
| TurtD1 | N. Dakota Geol. Surv. uncat. | Sentinel Butte Fm (Ft. Union Grp) | Paleocene | 57,000 | plastominid | 0.31 | 4.4 |
| TurtB10 | USNM 508564 | Aquia Fm, Liverpool Point, Charles Co., MD | Paleocene | 59,000 | UID turtle | 0.32 | 3.3 |
| TurtA6 | SMM uncat | Hell Creek Fm, Garfield Co., MT | Maastrichtian | 65,000 | UID turtle | 0.36 | 4.1 |
| TurtB1 | USNM 508562 | Chronister Site, Bollinger Co., MO | Campanian | 75,000 | UID turtle | 0.28 | 3.6 |
| TurtA7 | TMP uncat | Dinosaur Park Formation, Dinosaur Provincial Park, Alberta | Campanian | 75,000 | UID turtle | 0.36 | 4.8 |
| Mammals | | | | | | | |
| Deer tooth | ----- | Northern Indiana | Holocene | 0.001 | *Odocoileus virginianus* | 0.26 | 24.3 |
| Deer rib | ----- | Northern Indiana | Holocene | 0.001 | *Odocoileus virginianus* | 0.39 | 39.8 |
| Peccary tooth | ----- | Unknown | Holocene | 0.001 | *Tayassu tajacu* | 0.46 | 28.3 |
| Ungulate tooth | INSM uncat | Pipe Creek Sinkhole | Early Pliocene | 5000 | UID ungulate | 0.33 | 4.2 |
| Large mammal ?rib | INSM uncat | Pipe Creek Sinkhole | Early Pliocene | 5000 | UID ?large mammal | 0.33 | 5.1 |

specimen age; for about the first 14,000 years of aging, the organic content of bone (as measured by LOI) decreases as apatite crystallinity increases (cf. Tuross *et al*., 1989; Person *et al*., 1995; Sillen and Parkington, 1996; Hedges, 2002; Trueman and Martill, 2002). Plotting FWHM and LOI individually against specimen age (Figs. 8, 9) shows crystallinity increasing (FWHM decreasing) and LOI decreasing rapidly from modern turtle shell through archaeological samples to Late Pleistocene specimens, after which there is relatively little change. PCS bone shows values of LOI and FWHM typical of very old (pre-Pleistocene) bone.

## MICROBIAL ALTERATION OF PIPE CREEK SINKHOLE BONE

Some PCS bones that lack crystalline filling of pore spaces are dotted by hemispherical, often paired structures about 80 microns across (Fig. 10). These hemispheroids are fairly regular in shape, and have sharp contacts with the bone. Their sideritic composition (Table 2) differs from that of PCS bone, but is similar to that of material found in bone pore spaces.

Microscopic calcium carbonate, phosphatic, and siliceous spheroids, hemispheroids, dumbbells, and rods are created as by-products of bacterial metabolism in microbial mats and rapidly decaying organic matter (Buczynski and Chafetz, 1991; Chafetz and Buczynski, 1992; Briggs and Kear, 1994; Schmitz and Ernst, 1994; Briggs and Wilby, 1996; Hof and Briggs, 1997; Sageman *et al*., 1999; Renesto, 2005). Soft-part preservation of animal fossils in the famous Eocene Messel lake deposits of Germany was ac-

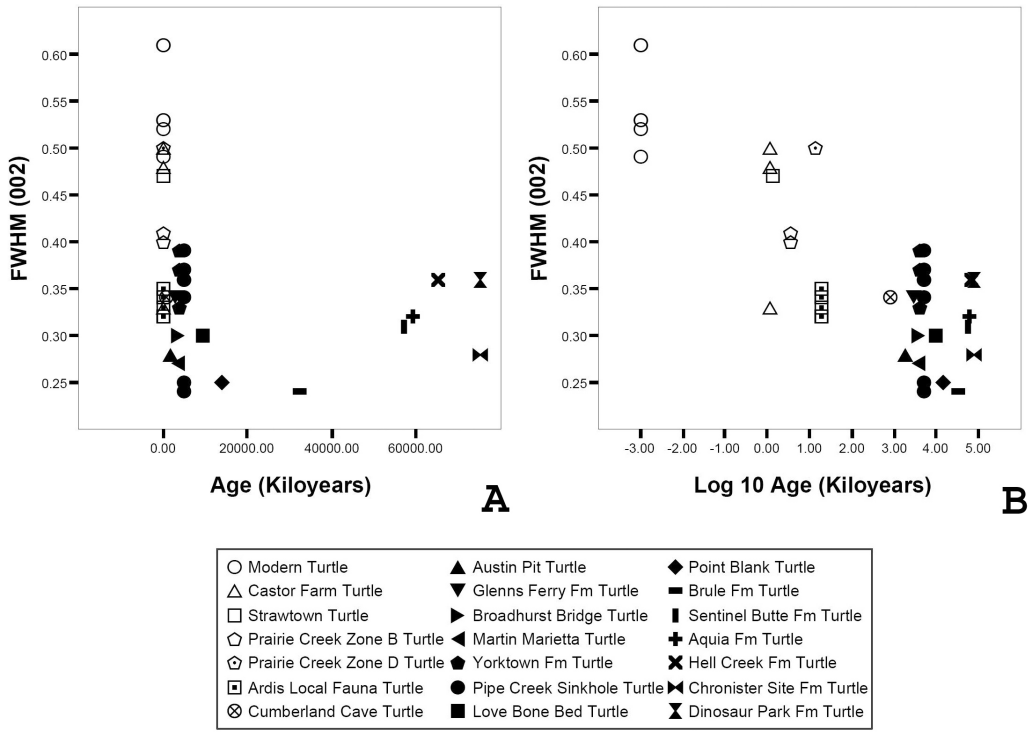


**Fig. 8.** Crystallinity (FWHM) of Pipe Creek Sinkhole turtle and tortoise shell compared with that of chelonian shell material from other sites of varying age (Table 5). **A,** Age of site in arithmetic units. **B**, Age of site in logarithmic units. Open symbols = modern samples; symbols with dots inside = samples from sites between 10,000 and 100,000 years age; circle with cross inside = sample from site between 100,000 and 1 million years old; solid symbols = samples from sites more than 1 million years old. The number of distinct points in the graph is less than the total sample size due to identical values for some specimens from the same site (Table 5).

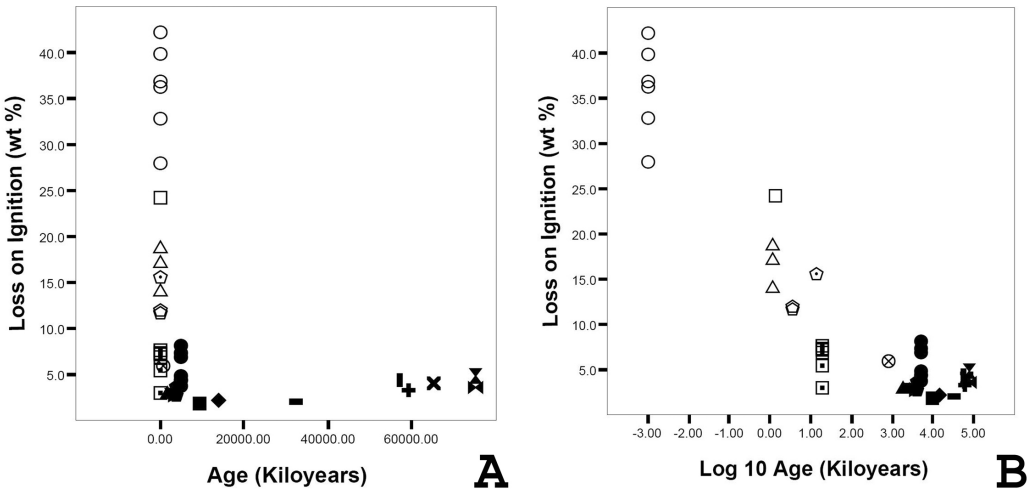


**Fig. 9.** Loss on ignition (LOI) of Pipe Creek Sinkhole turtle and tortoise shell compared with that of chelonian shell from other sites of varying age (Table 5). **A**, Age of site expressed in arithmetic units. **B**, Age of site expressed in logarithmic units. Symbols as in Fig. 8.

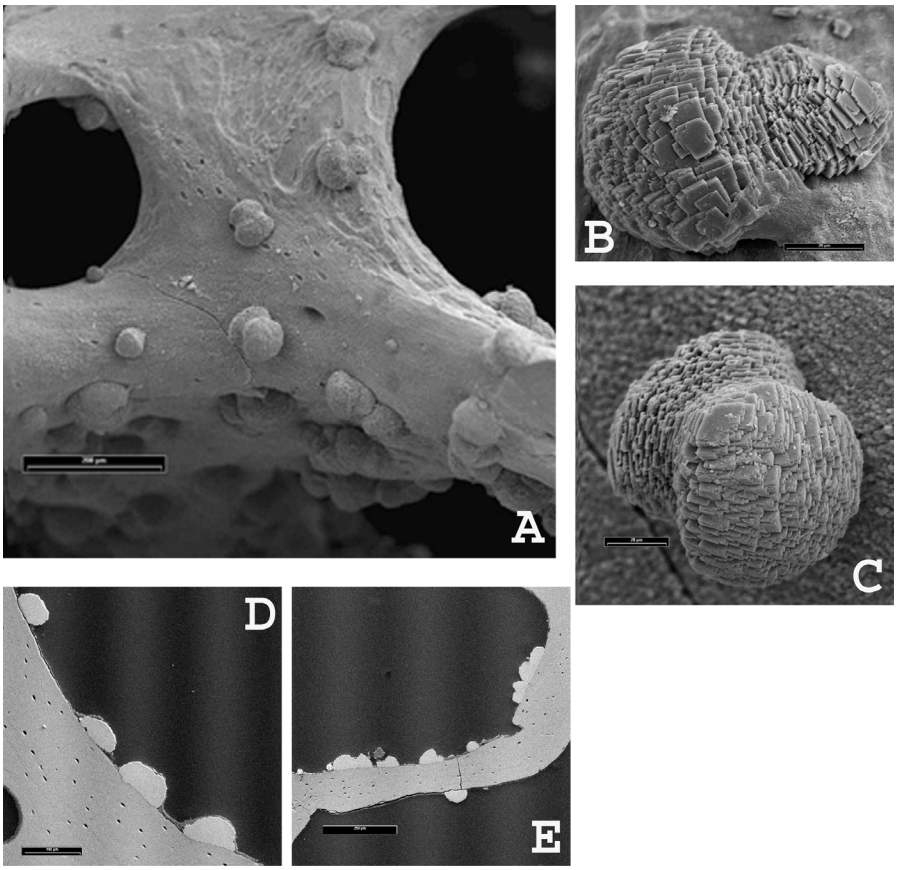


**Fig. 10.** SEM images of hemispheroidal structures on the trabecular bone of the interior of a large mammal ?rib (Tables 2, 5). **A-C**, Intact hemispheroids. **D-E**, Cross sections of bone showing sharp contacts between trabecular bone and the hemispheroids. Scale bars = 20 microns (**B, C**), 100 microns (**D**), 200 microns (**E**) or 250 microns (**A**).

complished by precipitation of siderite and pyrite in response to micro-scale, bacterially-generated chemical changes in water chemistry (Wuttke, 1992).

It therefore seems likely that the sideritic PCS hemispheroids were generated as a consequence of bacterial decomposition of organic matter in the bone interior (cf. Clarke and Barker, 1993; Clarke, 1994; Elorza *et al*., 1999; Carpenter, 2005), probably very early in diagenesis; in experimental studies of decomposition of crustaceans (e.g. Briggs and Kear, 1994), precipitation of calcium carbonate crystal bundles began within days of the animal's death. The PCS hemispheroids may have formed directly as siderite, or alternatively as later replacements of calcium carbonate precursors.

A different indication of possible microbial alteration of the same bone is seen in the "vermicular" texture of the external edge of the bone cortex (Fig. 11), comprising numerous irregular, curving, and possibly branching tunnels. These structures closely resemble Type 1 Wedl tunnels in size, shape, and location in the bone (Hackett, 1981; Trueman and Martill, 2002); such tunnels are thought to be made by fungi attacking bone material for its organic content. The chemical composition of bone at the vermicular edge of the ?rib does not differ from that of unaltered bone deeper in the cortex (Table 2). Although our preliminary observations suggest that PCS bone has not been greatly affected by such microbial attack (cf. Hedges and Millard, 1995; Trueman and Martill, 2002; Chinsamy-Turan, 2005 for fossil bones more generally), the fact that it did occur suggests that a systematic survey of bones from the site might yield interesting information about its taphonomic and early diagenetic history.

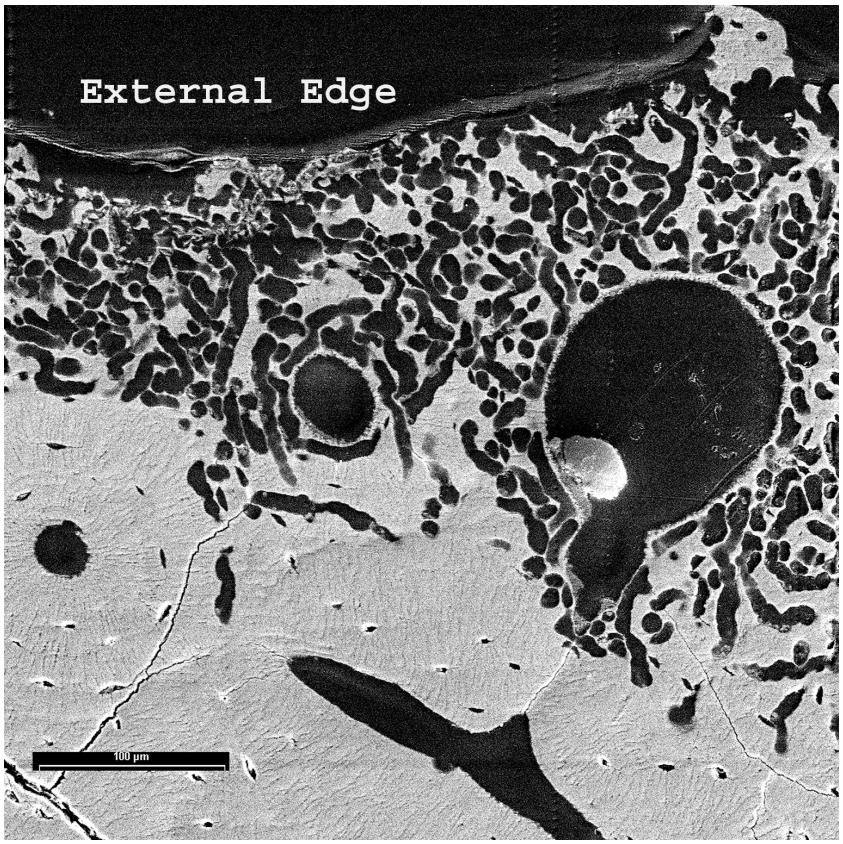


**Fig. 11.** SEM image showing "vermicular" texture of the outer part of the cortex of a large mammal ?rib (Tables 2, 5). Scale bar = 100 microns.

# DISCUSSION

## PALEOENVIRONMENTAL CONDITIONS DURING PCS BONE DIAGENESIS

PCS bone is very typical of fossil bone in terms of its chemistry, crystallinity, and degree of post-mortem biological alteration. The only unusual feature of PCS bone is its general lack of permineralization of large pore spaces within the bone.

Where infilling has occurred, the material involved is siderite, a permineralizing material often found in fossil bones of terrestrial vertebrates (Clarke and Barker, 1993; Pfretzschner, 2000b; Trueman *et al*., 2003; Clarke, 2004). The occurrence of siderite, both within bone pore spaces and in the abundant nodules found in the otherwise unconsolidated PCS fossiliferous layer, indicates the presence of ample Fe sources (presumably groundwater) in the sinkhole environment and its vicinity, as does the significant amount of terra rossa beneath and adjacent to the fossiliferous layer in the sinkhole (cf. Houston *et al*., 1966; Olson *et al*., 1980; Stephan, 1997; Pretzschner, 2000b). Siderite commonly forms in freshwater environments (often as concretions) characterized by low Eh, slightly alkaline pH, high concentrations of sulfur, and a high concentration of iron relative to that of calcium (Berner, 1971; Clarke and Barker, 1993). Such conditions could readily have occurred in organic-rich sediments of a sinkhole pond in a warm environment. The slightly alkaline conditions under which siderite forms would be ideal for bone preservation, and the generally good preservation of PCS bones further suggests that the pond sediments in which they were buried remained saturated during early diagenesis, and did not experience routine fluctuations in water content of the kind that apparently enhance microbial degradation of bone (Nicholson, 1996; Nielsen-Marsh and Hedges, 2000; Hedges, 2002). This may indicate that the pond was, for some unknown interval, "permanent" rather than intermittent – as also indicated by the abundant fossils of aquatic plants and animals in the PCS fossil assemblage (Farlow *et al*., 2001).

## CHANGES IN BONE CRYSTALLINITY AS A PROXY FOR SITE AGE

Bartsiokas and Middleton (1992) suggested that numerical indices of bone crystallinity could be used to determine the relative ages of archaeological and paleontological bone samples up to ages of about one million years. Sillen and Parkington (1996) likewise found a relationship between bone crystallinity and age, but only for bones up to about 20,000 years old. Over a time scale of thousands to millions of years, Person *et al*. (1995, 1996), however, found no relationship between bone crystallinity and age (also see Hedges and Millard, 1995), and argued that crystallinity changes occur in the earliest phases of inorganic diagenesis.

For turtle shell from pre-late Pleistocene sites, our data are consistent with the results of Person *et al*. (1995, 1996) in showing no relationship between bone crystallinity and age. However, for late Pleistocene and younger specimens, our data are consistent with the observations of Bartsiokas and Middleton (1992) and Sillen and Parkington (1996) for mammalian bone. As with the mammalian bone studied by those workers, our turtle shell material showed a clear increase in bone crystallinity with age. With more intense sampling of archaeological and relatively young Pleistocene sites, it might therefore be possible to create a quantitative "chelonistratigraphy" based on measurements of turtle shell bone crystallinity.

# ACKNOWLEDGMENTS

We acknowledge with pleasure the efforts of Ron Richards, Rex Garniewicz, Michele Greenan, Bill Wepler, and other staff of the Indiana State Museum in excavating the Pipe Creek Sinkhole. We thank R. Benton,M. Brett-Surman, D. Briggs, N. Clark, G. Darrough, S. Godfrey, F. Grady, J. Hoganson, R.

Hulbert, L. Knight, E. Lundelius, R. Mccullough, D. Parris, D. Prothero, R. Purdy, R. Richards, J. Sunderman, C. Trueman, and L. Ward for helpful discussions and/or access to specimens. T. Reece assisted in preliminary laboratory work for this project. We thank P. Higgins, L. L. Jacobs, and C. B. Wood for helpful reviews of our manuscript. This research was supported by NSF grant EAR-0207182 to Farlow.

# 미국 인디아나주 Grant County 신제3기 Pipe Creek Sinkhole에서 산출된 화석 뼈의 보존상태

**James O. Farlow and Anne Argast**

*Department of Geosciences, Indiana-Purdue University, 2101 East Coliseum Boulevard, Fort Wayne, IN 46805, U.S.A.*

**요 약:** 미국 인디아나주 Grant County의 Pipe Creek Sinkhole (PCS)에서 산출된 화석 군집은 신제3기의 크고 작은 다양한 육상, 수상의 척추동물의 풍부한 뼈를 보존하고 있다. PCS 뼈의 속성작용을 조사하기 위해 주사전자현미경, X선 회절 분석, 에너지 분산 X선 분석 그리고 연소 후 무게 감소 측정 등 몇 가지 기술을 사용하였다. 대부분 PCS 뼈는 외부에 거의 풍화가 없다. 내부적으로도 잘 보존되어 있지만 최소한 한 개의 뼈는 피질에 박테리아의 영향을 조금 받았다는 것을 보여준다. PCS 뼈의 화학분석은 보통의 뼈와 다르지 않다. 뼈 apatite는 francolite이다. PCS 뼈는 소량의 망간과 철을 포함하는데 뼈 구멍의 대부분은 결정질로 채워져 있지는 않지만 능철광 성분으로 채워진 구멍에서는 풍부하게 나타난다. 아마도 박테리아 기원의 미세한 능철광의 "반구형" (흔히 짝을 이룸)들이 어떤 PCS 뼈의 trabecular 표면에서 풍부하게 나타난다. 능철광은 수많은 결핵체와 완전히 고화되지 않은 PCS 화석층에서 풍부하다. PCS bone apatite는 현생 뼈보다 더 큰 결정질을 보이며 Full Width Half Maximum Values of the $d_{002}$ apatite peak는 다른 화석지의 뼈에서 보이는 것과 유사하다.

**주요어:** 보존, 화석뼈, Pipe Creek Sinkhole, 신제3기, Indiana

## REFERENCES

Ayliffe, L. K., Chivas, A. R. and Leakey, M. G. 1994. The retention of primary oxygen isotope compositions of fossil elephant skeletal phosphate. Geochimica et Cosmochimica Acta 58: 5291-5298.

Badone, E. and Farquhar, R. M. 1982. Application of neutron activation analysis to the study of element concentration and exchange in fossil bones. Journal of Radioanalytical Chemistry 69: 291-311.

Barker, M. J., Clarke, J. B. and Martill, D. M. 1997. Mesozoic reptile bones as diagenetic windows. Bulletin Societe Gèologique de France 168: 535-545.

Bartsiokas, A. and Middleton, A. P. 1992. Characterization and dating of recent and fossil bone by x-ray diffraction. Journal of Archaeological Science 19: 63-72.

Behrensmeyer, A. K., Western, D. and Boaz, D. E. D. 1979. New perspectives in vertebrate paleoecology from a Recent bone assemblage. Paleobiology 5: 12-21.

Bell, L. S., Skinner, M. F. and Jones, S. J. 1996a. The speed of post mortem change to the human skeleton and its taphonomic significance. Forensic Science International 82: 129-140.

Bell, M., Fowler, P. J. and Hillson, S. W. (eds.). 1996b. The Experimental Earthwork Project, 1960-1992. CBA Research Report, Council for British Archaeology, 267 pp.

Berna, F., Matthews, A. and Weiner, S. 2004. Solubilities of bone mineral from archaeological sites: the recrystallization window. Journal of Archaeological Science 21: 867-882.

Berner, R. A. 1971. Principles of Chemical Sedimentology. McGraw-Hill, New York, 240 pp.

Bocherens, H., Tresset, A., Weidemann, F., Giligny, F., Lafage, F., Lanchon, Y. and Mariotti, A. 1997. Diagenetic evolution of mammal bones in two French Neolithic sites. Bulletin Societe Geologique de France 168: 555-564.

Briggs, D. E. G. and Kear, A. J. 1994. Decay and mineralization of shrimps. Palaois 9: 431-456.

Briggs, D. E. G. and Wilby, P. R. 1996. The role of the calcium carbonate-calcium phosphate switch in the mineralization of soft-bodied fossils. Journal of the Geological Society, London 153: 665-668.

Brinkman, D. L. and Conway, F. M. 1985. Textural and mineralogical analysis of a *Stegosaurus*(Reptilia: Ornithischia) plate. Compass 63(1): 1-5.

Brophy, G. P. and Nash, J. T. 1968. Compositional, infrared, and x-ray analysis of fossil bone. American Mineralogist 53: 445-454.

Buczynski, C. and Chafetz, H. S. 1991. Habit of bacterially induced precipitates of calcium carbonate and the influence of medium viscosity on mineralogy. Journal of Sedimentary Petrology 61: 226-233.

Carpenter, K. 2005. Experimental investigation of the role of bacteria in bone fossilization. Neues Jahrbuch für Geologie und Palaöntologie Abhandlungen 2005: 83-94.

Chafetz, H. S. and Buczynski, C. 1992. Bacterially induced lithification of microbial mats. Palaios 7: 277-293.

Chang, L. L., Howie, R. A. and Zussman, J. 1998. Rock-Forming Minerals, Non-Silicates: Sulphates, Carbonates, Phosphates, Halides. Volume 5B, second edition. The Geological Society, London, 383 pp.

Child, A. M. 1995a. Microbial taphonomy of archaeological bone. Studies in Conservation 40: 19-30.

Child, A. M. 1995b. Towards an understanding of the microbial decomposition of archaeological bone in the burial environment. Journal of Archaeological Science 22: 165-174.

Chinsamy-Turan, A. 2005. The Microstructure of Dinosaur Bone: Deciphering Biology with Fine-Scale Techniques. Johns Hopkins University Press, Baltimore, MD, 216 pp.

Chipera, S. J. and Bish, D. L. 1991. Applications of X-ray diffraction crystallite size/strain analysis to *Seismosaurus* dinosaur bone. Advances in X-Ray Analysis 34: 473-482.

Clarke, J. B. 1994. Authigenic minerals in vertebrate fossils from the Wealden Group (Lower Cretaceous) of the Isle of Wight. Geological Curator 6: 11-15.

Clarke, J. B. 2004. A mineralogical method to determine cyclicity in the taphonomic and diagenetic history of fossilized bones. Lethaia 37: 281-284.

Clarke, J. B. and Barker, M. J. 1993. Diagenesis in *Iguanodon*bones from the Wealden Group, Isle of Wight, southern England. Kaupia 2: 57-65.

Cook, S. F. 1951. The fossilization of human bone: calcium, phosphate, and carbonate. University of California Publications in American Archaeology and Ethnology 40: 263-279.

Damuth, J. 1982. Analysis of the preservation of community structure in assemblages of fossil mammals. Paleobiology 8: 434-446.

Davis, P. G. 1997. The bioerosion of bird bones. International Journal of Osteoarchaeology 7: 388-401.

Denys, C. 2002. Taphonomy and experimentation. Archaeometry 44: 469-484.

Denys, C., Williams, C. T., Dauphin, Y., Andrews, P. and Fernandez-Jalvo, Y. 1996. Diagenetical changes in Pleistocene small mammal bones from Olduvai Bed I. Palaeogeography, Palaeoclimatology, Palaeoecology 126: 121-134.

Downing, K. F. and Park, L. E. 1998. Geochemistry and early diagenesis of mammal-bearing concretions from the Sucker Creek Formation (Miocene) of southeastern Oregon. Palaios 13: 14-27.

Dowsett, H. J. and Wiggs, L. B. 1992. Planktonic foraminiferal assemblage of the Yorktown Formation, Virginia, USA. Micropaleontology 38: 75-86.

Elorza, J., Astibia, H., Murelaga, X. and Pereda-Suberbiola, X. 1999. Francolite as a diagenetic mineral in dinosaur and other Upper Cretaceous reptile bones (Laño Iberian Peninsula): microstructural, petrological and geochemical features. Cretaceous Research 20: 169-187.

Farlow, J. O., Sunderman, J. A., Havens, J. J., Swinehart, A. L., Holman, J. A., Richards, R. L., Miller, N. G., Martin,

R. A., Hunt, R. M., Jr., Storrs, G. W., Curry, B. B., Fluegeman, R. H., Dawson, M. R. and Flint, M. E. T. 2001. The Pipe Creek Sinkhole Biota, a diverse late Tertiary continental fossil assemblage from Grant County, Indiana. American Midland Naturalist 145: 367-378.

Fernández-Jalvo, B., Sánchez-Chillón, P., Andrews, S., Fernández-López and Alcalá Martínez, L. 2002. Morphological taphonomic transformations of fossil bones in continental environments, and repercussions on their chemical composition. Archaeometry 44: 353-361.

Garland, A. N. 1987. A histological study of archaeological bone decomposition; pp. 109-126 In Boddington, A., Garland, A. N. and Janaway, R. C. (eds.), Death, Decay and Reconstruction: Approaches to Archaeology and Forensic Science. Manchester University Press, Manchester, U.K.

Gordon, C. C. and Buikstra, J. E. 1981. Soil pH, bone preservation, and sampling bias at mortuary sites. American Antiquity 46: 566-571.

Grupe, G. and Dreses-Werringloer, U. 1993. Decomposition phenomena in thin sections of excavated human bones; pp. 27-36 In Grupe, G. and Garland, A. N. (eds.), Histology of Ancient Human Bone: Methods and Diagnosis. Springer-Verlag, Berlin.

Grupe, G. and Piepenbrink, H. 1989. Impact of microbial activity on trace element concentrations in excavated bones. Applied Geochemistry 4: 293-298.

Hackett, C. J. 1981. Microscopical focal destruction (tunnels) in excavated human bones. Medicine, Science, and the Law 21: 243-265.

Hanson, D. B. and Buikstra, J. E. 1987. Histomorphological alteration in buried human bone from the lower Illinois Valley: implications for palaeodietary research. Journal of Archaeological Science 14: 549-563.

Hedges, R. E. M. 2002. Bone diagenesis: an overview of process. Archaeometry 44: 319-328.

Hedges, R. E. M. and Millard, A. R. 1995. Measurements and relationships of diagenetic alteration of bone from three archaeological sites. Journal of Archaeological Science 22: 201-209.

Henderson, J. 1987. Factors determining the state of preservation of human remains; pp. 43-54 In Boddington, A., Garland, A. N. and Janaway, R. C. (eds.), Death, Decay and Reconstruction: Approaches to Archaeology and Forensic Science. Manchester University Press, Manchester, U.K.

Hof, C. H. J. and Briggs, D. E. G. 1997. Decay and mineralization of mantis shrimps (Stomatopoda: Crustacea) – a key to their fossil record. Palaios 12: 420-438.

Holman, J. A. 2000. Fossil snakes of North America. Indiana University Press, Bloomington, IN, 357 pp.

Holman, J. A. 2003. Fossil frogs and toads of North America. Indiana University Press, Bloomington, IN, 246 pp.

Holman, J. A. and Richards, R. L. 1993. Herpetofauna of the Prairie Creek Site, Daviess County, Indiana. Proceedings of the Indiana Academy of Science 102: 115-131.

Houston, R. S., Toots, H. and Kelley, J. C. 1966. Iron content of fossil bones of Tertiary age in Wyoming correlated with climatic change. University of Wyoming Contributions to Geology 5: 1-18.

Hubert, J. F., Panish, P. T., Chure, D. J. and Prostak, K. S. 1996. Chemistry, microstructure, petrology, and diagenetic model of Jurassic dinosaur bones, Dinosaur National Monument, Utah. Journal of Sedimentary Research 66: 531-547.

Jans, M. M. E., Kars, H., Nielsen-Marsh, C. M., Smith, C. I., Nord, A. G., Arthur, P. and Earl, N. 2002. *In situ* preservation of archaeological bone: a histological study within a multidisciplinary approach. Archaeometry 44: 343-352.

Joshi, R. V. and Kshirsagar, A. A. 1986. Chemical Studies of Archaeological Bones from India: Fluorine and Fossilization Process. Deccan College Postgraduate and Research Institute, Poona, India, 85 pp.

Karkanas, P., Bar-Yosef, O., Goldberg, P. and Weiner, S. 2000. Diagenesis in prehistoric caves: the use of minerals that form *in situ* to assess the completeness of the archaeological record. Journal of Archaeological Science 27: 915-929.

Kohn, M. J. and Cerling, T. E. 2002. Stable isotope compositions of biological apatite. Reviews in Mineralogy and Geochemistry 48: 455-488.

Kurtén, B., and Anderson, E. 1980. Pleistocene Mammals of North America. Columbia University Press, New York, 442 pp.

Lee-Thorp, J. 2002. Two decades of progress towards understanding fossilization processes and isotopic signals in calcified tissue minerals. Archaeometry 44: 435-446.

Lee-Thorp, J. A. and Van der Merwe, N. J. 1991. Aspects of the chemistry of modern and fossil biological apatites. Journal of Archaeological Science 18: 343-354.

Locock, M., Currie, C. K. and Gray S. 1992. Chemical changes in buried animal bone: data from a postmedieval assemblage. International Journal of Osteoarchaeology 2: 297-304.

Martill, D. M. 1991. Bones as stones: the contribution of vertebrate remains to the lithologic record; pp. 270-292 In Donovan, S. K. (ed.), The Process of Fossilization. Columbia University Press, New York.

Martin, R. A., Goodwin, H. T. and Farlow, J. O. 2002. Late Neogene (Late Hemphillian) rodents from the Pipe Creek Sinkhole, Grant County, Indiana. Journal of Vertebrate Paleontology 22: 137-151.

Matsu'ura, S. 1982. A chronological framing for the Sangiran hominids – fundamental study by the fluorine dating method. Bulletin National Science Museum, Tokyo Series D 8: 1-53.

McCullough, R. G. (ed.). 2005. Late Prehistoric Archaeology of a Frontier. Indiana-Purdue University Fort Wayne-Archaeological Survey Reports of Investigations 502, 272 pp.

Metzger, C. A., Terry, D. O. Jr. and Grandstaff, D. E. 2004. Effect of paleosol formation on rare earth element signatures in fossil bone. Geology 32: 497-500.

Michel, V., Ildefonse, Ph. and Morin, G. 1996.Assessment of archaeological bone and dentine preservation from Lazaret Cave (Middle Pleistocene) in France. Palaeogeography, Palaeoclimatology, Palaeoecology 126: 109-119.

Moore, D. M. and Reynolds, R. C. Jr. 1997. X-Ray Diffraction and the Identification and Analysis of Clay Minerals, second edition. Oxford University Press, Oxford, U.K., 378 pp.

Neill, W. T. 1957. The rapid mineralization of organic remains in Florida, and its bearing on supposed Pleistocene records. Quarterly Journal of the Florida Academy of Sciences 20: 1-13.

Newesly, H. 1989. Fossil bone apatite. Applied Geochemistry 4: 233-245.

Nicholson, R. A. 1996. Bone degradation, burial medium and species representation: debunking the myths, an experiment-based approach. Journal of Archaeological Science 23: 513-533.

Nielsen-Marsh, C. M. and Hedges, R. E. M. 2000. Patterns of diagenesis in bone I: the effects of site environments. Journal of Archaeological Science 27: 1139-1150.

Nriagu, J. O. 1983. Rapid decomposition of fish bones in Lake Erie sediments. Hydrobiologica 106: 217-222.

Oakley, K. P. 1949. The fluorine dating method. Yearbook of Physical Anthropology 5: 44-52.

Olson, C. G., Ruhe, R. V. and Mausbach, M. J. 1980. The terra rossa limestone contact phenomena in karst, southern Indiana. Soil Science Society of America Journal 44: 1075-1079.

Paine, G. 1937. Fossilization of bone. American Journal of Science 234: 148-157.

Parker, R. B., Murphy, J. W. and, Toots, H. 1974. Fluorine in fossilized bone and tooth: distribution among skeletal tissues. Archaeometry 16: 98-102.

Parker, R. B. and Toots, H. 1974. Minor elements in fossil bone: application to Quaternary samples. Geological Survey of Wyoming, Reports of Investigations 10: 74-77.

Parker, R. B. and Toots, H. 1980. Trace elements in bones as paleobiological indicators; pp. 197-207 In Behrensmeyer, A. K. and Hill, A. P. (eds.), Fossils in the Making: Vertebrate Taphonomy and Paleoecology. University of Chicago Press, Chicago.

Pate, F. D. and Hutton, J. T. 1988. The use of soil chemistry data to address post-mortem diagenesis in bone mineral. Journal of Archaeological Science 15: 729-739.

Person, A., Bocherens, H., Mariotti, A. and Renard, M. 1996. Diagenetic evolution and experimental heating of bone phosphate. Palaeogeography, Palaeoclimatology, Palaeoecology 126: 135-149.

Person, A., Bocherens, H., Saliège, J.-F., Paris, F., Zeitoun, V. and Gérard, M. 1995. Early diagenetic evolution of bone phosphate: an x-ray diffractometry analysis. Journal of Archaeological Science 22: 211-221.

Pfretzschner, H.-U. 2000a. Microcracks and fossilization of Haversian bone. Neues Jahrbuch für Geologie und Palaöntologie Abhandlungen 216: 413-432.

Pfretzschner, H.-U. 2000b. Pyrite formation in Pleistocene bones – a case of very early mineral formation during diagenesis. Neues Jahrbuch für Geologie und Palaöntologie Abhandlungen 217: 143-160.

Pfretzschner, H.-U. 2001a. Iron oxides in fossil bone. Neues Jahrbuch für Geologie und Palaöntologie Abhandlungen

220: 417-429.
Pfretzschner, H.-U. 2001b. Pyrite in fossil bone. Neues Jahrbuch für Geologie und Palaöntologie Abhandlungen 220: 1-23.
Pfretzschner, H.-U. 2004. Fossilization of Haversian bone in aquatic environments. Comptes Rendus Palevol 3: 605-616.
Piepenbrink, H. 1986. Two examples of biogenous dead bone decomposition and their consequences for taphonomic interpretation. Journal of Archaeological Science 13: 417-430.
Piepenbrink, H. 1989. Examples of chemical changes during fossilization. Applied Geochemistry 4: 273-280.
Price, T. D. 1989. Multi-element studies of diagenesis in prehistoric bone; pp. 126-154 In Price, T. D. (ed.), The Chemistry of Prehistoric Human Bone. Cambridge University Press, Cambridge, U.K.
Quattropani, L., Charlet, L., De Lumley, H. and Menu, M. 1999. Early Palaeolithic bone diagenesis in the Arago cave at Tautavel, France. Mineralogical Magazine 63: 801-812.
Reiche, I., Vignaud, C. and Menu, M. 2002. The crystallinity of ancient bone and dentine: new insights by transmission electron microscopy. Archaeometry 44: 447-459.
Renesto, S. 2005. A new specimen of *Tanystropheus* (Reptilia: Protorosauria) from the Middle Triassic of Switzerland and the ecology of the genus. Revista Italiana di Paleontologia Stratigrapfia 111: 377-394.
Rogers, A. F. 1924. Mineralogy and petrography of fossil bone. Bulletin Geological Society of America 35: 535-556.
Sageman, J., Bale, S. J., Briggs, D. E. K. and Parkes, R. J. 1999. Controls on the formation of authigenic minerals in association with decaying organic matter: an experimental approach. Geochimica et Cosmochimica Acta 63: 1083-1095.
Samoilov, V. S. and Benjamini, C. 1996. Geochemical features of dinosaur remains from the Gobi Desert, South Mongolia. Palaios 11: 519-531.
Schmitz, M. and Ernst, K. 1994. Microspheroidal objects within the Eocene Messel Formation (Messel Oilshale Pit/Germany). Kaupia 4: 13-19.
Schoeninger, M. J., Moore, K. M., Murray, M. L. and Kingston, J. D. 1989. Detection of bone preservation in archaeological and fossil samples. Applied Geochemistry 4: 281-292.
Schuffert, J. D., Kastner, M., Emanuele, G. and Jahnke, R. A. 1990. Carbonate-ion substitution in francolite: a new equation. Geochimica et Cosmochimica Acta 54: 2323-2328.
Sillen, A. 1989. Diagenesis of the inorganic phase of cortical bone; pp. 211-229 In Price, T. D. (ed.), The Chemistry of Prehistoric Human Bone. Cambridge University Press, Cambridge, U.K.
Sillen, A. and Parkington, J. 1996. Diagenesis of bones from Eland's Bay Cave. Journal of Archaeological Science 23: 535-542.
Smith, C. I., Nielsen-Marsh, C. M., Jans, M. M. E., Arthur, P., Nord, A. G. and Collins, M. J. 2002. The strange case of Apigliano: early 'fossilization'of Medieval bone in southern Italy. Archaeometry 44: 405-415.
Stephan, E. 1997. Patterns of chemical change in fossil bones and various states of bone preservation associated with soil conditions. Anthropozoologica 1997: 173-180.
Toots, H. 1963. The chemistry of fossil bones from Wyoming and adjacent states. University of Wyoming Contributions in Geology 2: 69-80.
Toots, H. and Parker, R. B. 1979. Factors affecting fluorine content of fossil bones and teeth. Contributions to Geology, University of Wyoming 18: 69-70.
Trueman, C. N. and Benton, M. J. 1997. A geochemical method to trace the taphonomic history of reworked bones in sedimentary settings. Geology 25: 263-266.
Trueman, C. N. and Martill, D. M. 2002. The long-term survival of bone: the role of bioerosion. Archaeometry 44: 371-382.
Trueman, C. N., Chenery, C., Eberth, D. A. and Spiro, B. 2003. Diagenetic effects on the oxygen isotope composition of bones of dinosaurs and other vertebrates recovered from terrestrial and marine sediments. Journal of the Geological Society, London 160: 895-901.
Tuross, N., Behrensmeyer, A. K. and Eanes, E. D. 1989a. Strontium increases and crystallinity changes in taphonomic and archaeological bone. Journal of Archaeological Science 16: 661-672.
Tuross, N., Behrensmeyer, A. K., Eanes, E. D., Fisher, L. W. and Hare, P. E. 1989b. Molecular preservation and crystallo-

graphic alterations in a weathering sequence of wildebeest bones. Applied Geochemistry 4: 261-270.

Van Der Meulen, A. J. 1978. *Microtus* and *Pitymys* (Arvicolidae) from Cumberland Cave, Maryland, with a comparison of some New and Old World species. Annals of Carnegie Museum 47: 1010-145.

Von Endt, D. W. and Ortner, D. J. 1984. Experimental effects of bone size and temperature on bone diagenesis. Journal of Archaeological Science 11: 247-253.

Waldron, T. 1987. The relative survival of the human skeleton: implications for palaeopathology; pp. 55-64 In Boddington, A., Garland, A. N. and Janaway, R. C. (eds.), Death, Decay and Reconstruction: Approaches to Archaeology and Forensic Science. Manchester University Press, Manchester, U.K.

Ward, L. W. 1985. Stratigraphy and characteristic mollusks of the Pamunkey Group (lower Tertiary) and the Old Church Formation of the Chesapeake Group – Virginia Coastal Plain. U.S. Geological Survey Professional Paper 1346, 78 pp.

Ward, L. W. and Powers, D. S. 1989. Tertiary Stratigraphy and Paleontology, Chesapeake Bay Region, Virginia and Maryland. Field Trip Guidebook T216, 28th International Geological Congress, American Geophysical Union, Washington, D.C., 64 pp.

White, E. M. and Hannus, L. A. 1983. Chemical weathering of bone in archaeological soils. American Antiquity 48: 316-322.

Williams, C. T. and Potts, P. J. 1988. Element distribution maps in fossil bones. Archaeometry 30: 237-247.

Woodburne, M. O. (ed.). 2004. Late Cretaceous and Cenozoic Mammals of North America: Biostratigraphy and Geochronology. Columbia University Press, New York, 391 pp.

Wuttke, M. 1992. Conservation – dissolution – transformation. On the behaviour of biogenic materials during fossilization; pp. 265-275 In Schaal, S. and Ziegler, W. (eds), Messel: An Insight into the History of Life and of the Earth. Clarendon Press, Oxford, U.K.

Zocco, T. G. and Schwartz, H. L. 1994. Microstructural analysis of bone of the sauropod dinosaur *Seismosaurus* by transmission electron microscopy. Palaeontology 37: 493-503.